Environmental Pollution 195 (2014) 218–225

Contents lists available at ScienceDirect

Environmental Pollution

journal homepage: www.elsevier.com/locate/envpol

Silver, zinc oxide and titanium dioxide nanoparticle ecotoxicity to bioluminescent *Pseudomonas putida* in laboratory medium and artificial wastewater

Florian Mallevre, Teresa F. Fernandes, Thomas J. Aspray*

School of Life Sciences, NanoSafety Research Group, Heriot-Watt University, Edinburgh EH14 4AS, Scotland, UK

ARTICLE INFO

Article history:
Received 4 July 2014
Received in revised form
28 August 2014
Accepted 2 September 2014
Available online 27 September 2014

Keywords:
Bacterial biosensor
Ecotoxicity
Nanoparticle
Bioreporter
Pseudomonas putida
Wastewater

ABSTRACT

Bacteria based ecotoxicology assessment of manufactured nanoparticles is largely restricted to *Escherichia coli* bioreporters in laboratory media. Here, toxicity effects of model OECD nanoparticles (Ag NM-300K, ZnO NM-110 and TiO_2 NM-104) were assessed using the switch-off luminescent *Pseudomonas putida* BS566::luxCDABE bioreporter in Luria Bertani (LB) medium and artificial wastewater (AW). IC_{50} values ~4 mg L^{-1}, 100 mg L^{-1} and >200 mg L^{-1} at 1 h were observed in LB for Ag NM-300K, ZnO NM-110 and TiO_2 NM-104, respectively. Similar results were obtained in AW for Ag NM-300K (IC_{50} ~5 mg L^{-1}) and TiO_2 NM-104 (IC_{50} >200 mg L^{-1}) whereas ZnO NM-110 was significantly higher (IC_{50} >200 mg L^{-1}). Lower ZnO NM-110 toxicity in AW compared to LB was associated with differences in agglomeration status and dissolution rate. This work demonstrates the importance of nanoecotoxicological studies in environmentally relevant matrices.

1. Introduction

Manufactured nanoparticles (NPs), defined as anthropogenic materials exhibiting all three external dimensions at the nanoscale (*i.e.* between 1 and 100 nm), are being increasingly used in commercial products and industrial processes due to new or enhanced physico-chemical properties compared to their bulk counterparts (Ju-Nam and Lead, 2008). Despite offering benefits, the wide use of NPs has raised questions regarding their potential release and impact to humans and the environment (Peralta-Videa et al., 2011; Scown et al., 2010). However, toxicological and more specifically ecotoxicological studies with NPs are still limited and as such the potential adverse effects of NPs remain largely unknown. Consequently, whereas nanoparticle science is leading to new interfacial materials (*i.e.* materials birthed by meeting two different parent materials at the atomic level), nanoecotoxicological science currently lags behind in developing suitable tools and approaches for identifying fate and effect of parent materials (Kahru and Ivask, 2013; Kim et al., 2012; Klaine et al., 2008).

A key issue in the assessment of the safety of nanoparticles is the appropriateness of standard protocols (such as OECD or ISO) to assess nanoparticle hazard. In this study we focus on three of the most widely used NPs, namely silver (Ag), zinc oxide (ZnO) and titanium dioxide (TiO_2); inorganic NPs are of particular interest due to their physico-chemical properties. Ag is commonly used for its anti-microbial properties and is frequently incorporated in NP form in many products including clothes, paints and kitchen appliances (Chernousova and Epple, 2013). ZnO and TiO_2 are well known for their UV-protection and photo-catalytic properties, and are widely used in cosmetics, sunscreens and paints (Di Paola et al., 2012; Smijs and Pavel, 2011). These NPs are now available in a variety of forms, with various sizes, shapes, coatings, and thus different properties, and consequently fate and behaviour, challenging further the establishment of harmonised and reproducible nanoecotoxicological approaches as currently much debated in the scientific literature (Oomen et al., 2014; Paterson et al., 2011).

Given the above situation, bacteria, and notably genetically modified bacteria (GMB), represent particularly interesting screening tools already validated in ecotoxicology over the last two decades for drug and chemical testing (Girotti et al., 2008). A large number of GMB bioreporters have been developed to either 'switch-on' or 'switch-off' emitting a quantifiable signal, usually luminescence or fluorescence, in the presence of toxicant(s) or

* Corresponding author.
E-mail addresses: T.J.Aspray@hw.ac.uk, thomasaspray@gmail.com (T.J. Aspray).

http://dx.doi.org/10.1016/j.envpol.2014.09.002
0269-7491/

particular stress(es). Examples of applications with pesticides, pollutants, drugs or antibiotics, involving either pathogenic or non-pathogenic Gram positive or Gram negative GMB as inducible (switch-on) or constitutive (switch-off) bioreporters, are abundant (van der Meer and Belkin, 2010; Xu et al., 2013). Due to their ease of handling, rapid growth and potential to be compatible with field portable devices light-emitting GMB offer clear advantages for screening approaches in nanoecotoxicology as well (Holden et al., 2013; Sadik et al., 2009).

A few luminescent and fluorescent switch-off and switch-on GMB bioreporters have recently been used to either monitor the toxicity and evaluate inhibitory concentrations (Choi et al., 2008; Deryabin et al., 2012; Gogoi et al., 2006; Jiang et al., 2011; Sotiriou and Pratsinis, 2010) or to investigate nucleic acid, membrane, protein damage and oxidative stress associated to the toxicity (Bondarenko et al., 2013; Hwang et al., 2008; Li et al., 2013) of some silver, zinc, copper and titanium NPs or carbon nanotubes. This literature attests above all to the potential of light-emitting GMB based tools for NP testing. However so far, applications have been almost exclusively based on *Escherichia coli* bioreporters and restricted to NP testing in rich undefined laboratory media such as Luria Bertani (LB). A luminescent switch-off *Pseudomonas putida* has been recently proposed but only employed for silver testing in LB media (Dams et al., 2011). Therefore, although NPs are described as emerging contaminants given their widespread use and known to end up in the environment (*e.g.* in wastewaters and in soils due to sludge applications) (Eduok et al., 2013; Marcoux et al., 2013), reproducible approaches with relevant GMB suitable for testing in more relevant environmental matrices are scarce.

Consequently, in line with current needs in the assessment of hazard of manufactured nanoparticles the aims of this work were: 1) to assess the relative ecotoxicity of model OECD nanoparticles Ag NM-300K, ZnO NM-110 and TiO_2 NM-104 in Luria-Bertani medium and artificial wastewater using the *Pseudomonas putida* BS566::luxCDABE bioreporter (originally isolated from wastewater) and, 2) to relate ecotoxicity results to NP fate through their characterisation in the two matrices, specifically agglomeration status and dissolution rate.

2. Experimental

2.1. Materials

Silver (Ag NM-300K), zinc oxide (ZnO NM-110) and titanium dioxide (TiO_2 NM-104) OECD model NPs were obtained from the European Commission's Joint Research Centre (Ispra, Italy). Supplier related information is presented in Table 1. Ammonium sulphate ($(NH_4)_2SO_4$), calcium chloride ($CaCl_2$), D-glucose, di-sodium hydrogen orthophosphate (Na_2HPO_4), iron (III) chloride ($FeCl_3$), magnesium chloride ($MgCl_2$), potassium dihydrogen orthophosphate (KH_2PO_4), sodium chloride (NaCl), silver nitrate ($AgNO_3$), zinc sulphate ($ZnSO_4$), tryptone and yeast extract were purchased from Fisher Scientific UK Ltd. Kanamycin sulphate and *Pseudomonas* isolation agar were from Sigma–Aldrich Company UK Ltd. Silver and zinc pure single element standards were from Perkin Elmer UK Inc.

Table 1
Ag NM-300K, ZnO NM-110 and TiO_2 NM-104 supplier information.

	Appearance	Primary particle size (nm)	Mean particle size (nm)	Specific surface area ($m^2\ g^{-1}$)	Other information
Ag NM-300K	Suspension (brown)	15	15	N/A	Uncoated In dispersant*
ZnO NM-110	Powder (white)	42	150	13	Uncoated
TiO_2 NM-104	Powder (white)	20	67	60	Rutile Hydrophilic

N/A - not available.
* 4% each of Polyoxyethylene Glycerol Trioleate and Polyoxyethylene (20) Sorbitan mono-Laurat (Tween 20).

2.2. Methods

2.2.1. Bacterial bioreporter preparation

The constitutively luminescent (switch-off) *Pseudomonas putida* BS566::luxCDABE was used as bacterial bioreporter. *P. putida* BS566::luxCDABE was constructed by transposon (Tn5) mutagenesis based insertion of the full *lux* operon from *Photorhabdus luminescens*, along with a kanamycin resistance gene as marker, into the genome of a *P. putida* BS566 strain originally isolated from a wastewater treatment plant (Wiles et al., 2003). Bacterial bioreporters were maintained on *Pseudomonas* isolation agar plates supplemented with 100 mg L^{-1} of kanamycin. Prior to each experiment, bacterial bioreporters were pre-cultured overnight at 28 ± 2 °C under shaking conditions (140 rpm) to late exponential stage then freshly diluted in order to reach a final concentration per well of ~10^8 cfu mL^{-1} (early exponential phase) as previously described (Dams et al., 2011). Bacteria were pre-cultured either in LB laboratory rich medium (10.0 g L^{-1} of tryptone, 5.0 g L^{-1} of yeast extract, 5.0 g L^{-1} of NaCl, pH 7) or in AW consisting of AB mineral medium (2 g L^{-1} $(NH_4)_2SO_4$, 6 g L^{-1} Na_2HPO_4, 3 g L^{-1} KH_2PO_4, 3 g L^{-1} NaCl, 0.1 mM $CaCl_2$, 1 mM $MgCl_2$, 3 μM $FeCl_3$, pH 7) supplemented with 0.5% (w/v) of glucose as carbon source (Aspray et al., 2005). AB mineral medium with 0.5% glucose has been proposed as artificial wastewater due to being similar in composition to artificial wastewaters as described elsewhere (Martin et al., 2008; Shim et al., 2005).

2.2.2. Nanoparticle preparation

Ag NM-300K, ZnO NM-110 and TiO_2 NM-104 NPs were received conditioned under argon and preserved in the dark until use. Stock suspensions were freshly prepared in matrices of exposure (LB and AW) prior to each experiment, sonicated (2 × 8 min in a Kerry ultrasonic water bath at 38 ± 10 KHz), then serially diluted to give final concentrations per well ranging from 0 to 200 mg L^{-1} (*i.e.* 0, 0.781, 1.562, 3.125, 6.25, 12.5, 25, 50, 100, 200 mg L^{-1}), as previously described (Gaiser et al., 2013). Ag and Zn ions, applied as $AgNO_3$ and $ZnSO_4$, were prepared as above for final testing ranging from 0 to 25 mg L^{-1} and 0 to 200 mg L^{-1}, respectively.

2.2.3. Screening of nanoparticle ecotoxicity

Based on a switch-off approach the toxicity of Ag NM-300K, ZnO NM-110 and TiO_2 NM-104 NPs (as well as Ag and Zn ions) was tested in 96-well flat bottomed black microtitre plates (Greiner bio-one, Germany) on *Pseudomonas putida* BS566::luxCDABE by real time monitoring of the emitted luminescence evolution (*i.e.* reduction) with a SpectraMax M5 reader (Molecular Devices, USA). Assays were realised in 100% LB or 100% AW with final element and cell concentrations of 0–200 mg L^{-1} and 10^8 cfu mL^{-1}, respectively, in a final volume of 100 μL per well. Plates were incubated at 28 °C in the reader and the luminescence monitoring undertaken in a kinetic mode with measurements taken every 15 min for 120 min. Control wells containing cells without toxicant were used to determine ratios of luminescence defined as treated/untreated samples. Results arbitrarily expressed in Relative Light Units (RLU) against time (min) by the reader were transformed to percent Relative Luminescence (%RLU) and plotted against toxicant concentrations (mg L^{-1}) for selected time points (*e.g.* 0, 1, 2 h). Time point of 0 h corresponds to the first measure registered in a 5 min time window after exposure of bacterial bioreporters to the nanoparticles. NP toxicity was then expressed as IC_{50} when applicable.

2.2.4. Nanoparticle characterisation

2.2.4.1. Agglomeration. Agglomeration status of Ag NM-300K, ZnO NM-110 and TiO_2 NM-104 NPs were evaluated in LB and AW by dynamic light scattering (DLS) as well as by UV–visible spectrophotometry (UV–vis), both conducted with fresh NP preparations. Size distribution (*i.e.* z-average) was determined by DLS in dedicated clear disposable capillary cells (DTS1070) with a Nano Zetasizer (Malvern, UK) equipped with a 633 nm laser set at a scattering angle of 173°. UV–vis was conducted in clear disposable cuvettes (semi micro 1.5 mL, Kartell, UK) with an Evolution 600 spectrophotometer (Fisher Scientific, UK) between 300 nm and 800 nm in a scan mode with measures taken every 1 nm at a speed of 240 nm min^{-1}.

2.2.4.2. Dissolution. Dissolution rates of Ag NM-300K and ZnO NM-110 NPs were evaluated in LB and AW by atomic absorption spectroscopy (AAS) using an AAnalyst 200 Spectrometer (Perkin Elmer, UK) via the quantification of either Ag or Zn released ion concentration from each type of NP using dedicated lamps specific to each element (Lumina Hollow Cathode, diameter 50 mm). Briefly, NPs suspensions were prepared as described above and analysed immediately or incubated at room temperature (RT) for 1 h, respectively. Samples were pelleted by centrifugation (Avanti Centrifuge J-26XP, Beckman Coulter UK Ltd.) at 4 °C in 15 mL open-top polycarbonate tubes at 20 000 rpm (JA-25.15 rotor, Beckman Coulter UK Ltd.) for 30 min, as described elsewhere (Li et al., 2011; Zook et al., 2011). Supernatants were collected and used for AAS analysis without acidification. Dissolution rates were calculated as ratios between the AAS measured concentration of released element from NPs and the original prepared concentration of NPs. AAS was calibrated with Ag or Zn pure single element standards at concentrations of 0.156, 0.312, 0.625, 1.25, 2.5 and 5 mg L^{-1}. Uncentrifuged and unacidified Ag and ZnO NPs at 1 mg L^{-1} were also measured by AAS, validating preparation conditions (data not shown).

2.2.5. Data analysis

All presented results are mean ± standard error of the mean from three independent experiments with different batches of cells, suspensions of NPs and matrices. IC_{50} values were calculated by fitting a four parameter dose–response model to the logarithm of the concentration by weighted least squares with Prism software (GraphPad Software, USA). Size distribution (z-average) values were determined with Zetasizer Software (Malvern, UK). Data were tested for normality and homoscedasticity and found to comply with parametric requirements. Statistical significant differences between results were tested using a two-way analysis of variance (two-way ANOVA) followed by the multiple comparison Tukey test.

3. Results

3.1. Screening of nanoparticle ecotoxicity

Light output reductions over time by *P. putida* BS566::luxCDABE when exposed to a range of concentrations of Ag NM-300K, ZnO NM-110 and TiO_2 NM-104 NPs (from 0 to 200 mg L^{-1}) either in LB or in AW are shown in Fig. 1. Calculated IC_{50} values are presented in Table 2.

For Ag NM-300K, toxicity was apparent from 0 h (*i.e.* time point of 0 h corresponds to the first measure registered in a 5 min time window after exposure of bacterial bioreporters to the nanoparticles) in LB at higher concentrations (12.5–200 mg L^{-1}) (Fig. 1A.). After 1 h, toxicity was displayed at lower concentrations (*i.e.* below 12.5 mg L^{-1}) and remained consistent to 2 h of exposure (Fig. 1C. and E.). As Ag NM-300K was supplied in dispersant (Table 1), a dispersant only control was also tested which showed no toxic effects to *P. putida* BS566::luxCDABE (data not shown). In AW, comparable results were obtained (Fig. 1B., D. and F.). Based on derived IC_{50} values (Table 2), there was no significant difference in toxicity between 15 min and 2 h of exposure in either matrix. In addition, no cellular recovery phenomenon over time was observed (*i.e.* a recovery of the emitted luminescence due to regrowth of the

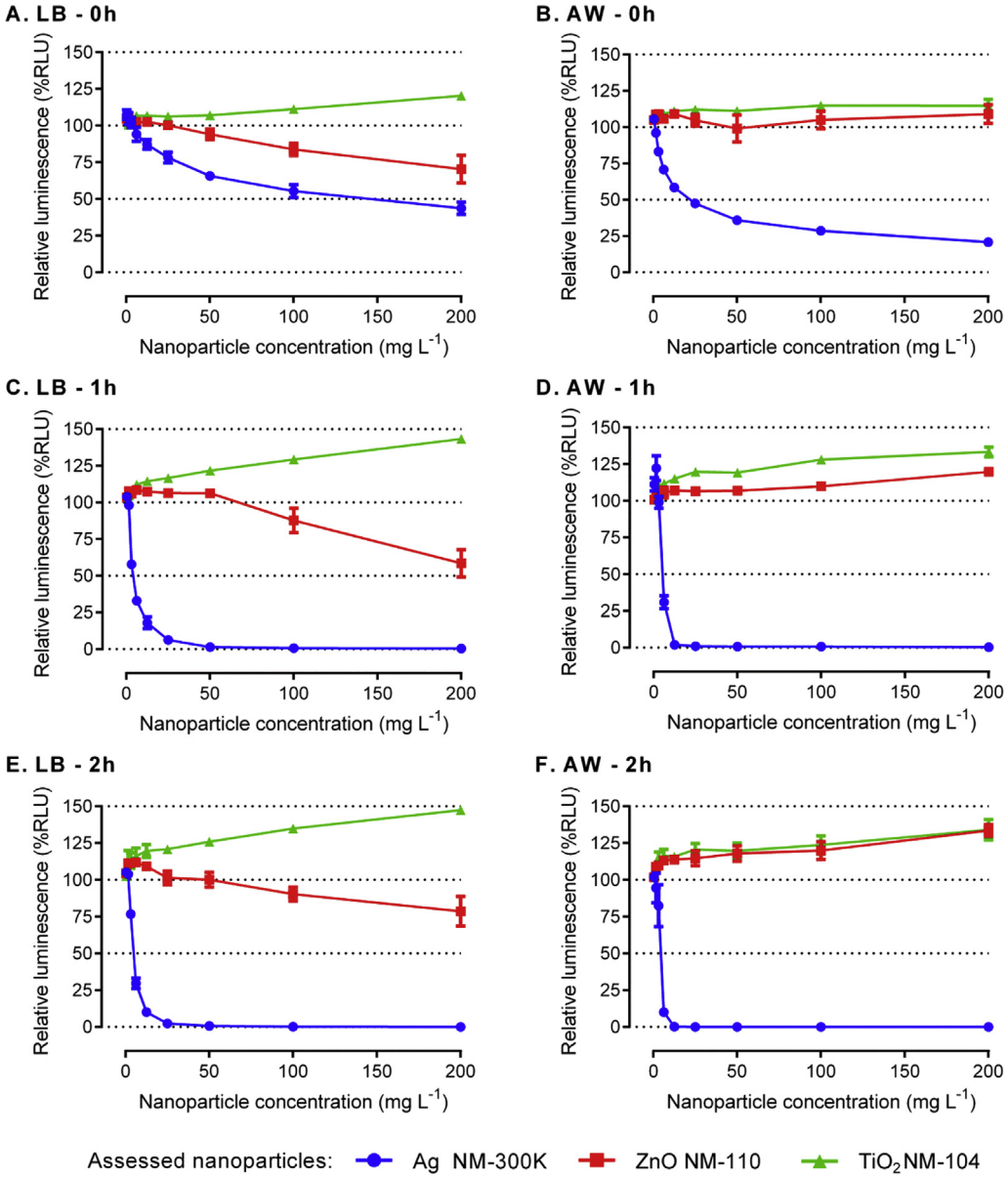

Fig. 1. Ag NM-300K, ZnO NM-110 and TiO_2 NM-104 toxicity on *P. putida* BS566::luxCDABE in Luria Bertani (LB) medium and artificial wastewater (AW). Relative luminescence output reductions by *P. putida* BS566::luxCDABE when challenged with 0–200 mg L^{-1} of Ag (blue circles), ZnO (red squares) and TiO_2 (green triangles) nanoparticles in LB (A., C. and E.) or in AW (B., D. and F.) for various time points (0 h, 1 h and 2 h, respectively). Data are mean ± standard error of the mean ($n = 3$). (For interpretation of the references to colour in this figure legend, the reader is referred to the web version of this article.)

Table 2
Ag NM-300K and ZnO NM-110 calculated IC_{50} on *P. putida* BS566::luxCDABE in Luria Bertani (LB) medium and artificial wastewater (AW).

		IC_{50} (mg L^{-1})					
		0 min	15 min	30 min	60 min	90 min	120 min
Ag NM-300K	LB	62.8 (±16.2)[c]	9.3 (±1.3)[ab]	4.8 (±0.3)[a]	3.8 (±0.1)[a]	4.0 (±0.1)[a]	4.0 (±0.2)[a]
	AW	32.0 (±4.9)[c]	13.8 (±1.5)[b]	6.4 (±0.4)[a]	5.0 (±0.7)[a]	4.4 (±0.9)[a]	4.0 (±0.8)[a]
ZnO NM-110	LB	58.8 (±6.1)[c]	79.8 (±1.3)[abc]	88.5 (±1.3)[abc]	100.4 (±2.3)[abc]	100.4 (±0.3)[ac]	ND[ab]
	AW	ND[c]					

Data are mean ± standard error of the mean ($n = 3$).
ND – IC_{50} were not determined due to non-observed toxicity (considered higher than 200 mg L^{-1}).
[a] Significantly different from the first time point ($p < 0.001$).
[b] Significantly different from the previous time point ($p < 0.05$).
[c] Significantly different from the other matrix ($p < 0.001$).

bacterial bioreporter population). In summary, toxic effects of Ag NM-300K were found to be similar in LB and AW and were observed from early stages of exposure. Comparatively, IC_{50} values at 1 h for Ag ions (applied as silver nitrate) were respectively 0.39 ± 0.05 mg L^{-1} and 0.36 ± 0.03 mg L^{-1} in LB and AW.

For ZnO NM-110, relative luminescence reduction patterns (Fig. 1, red curves) showed overall lower toxicity over time than was obtained for Ag. More specifically, ZnO NM-110 showed transient toxicity on *P. putida* BS566::luxCDABE in LB, characterised by IC_{50} values evolving from 58.8 ± 6.1 mg L^{-1} to 100.4 ± 2.3 mg L^{-1} for the first hour of exposure before becoming incalculable at 2 h (Table 2). ZnO NM-110 was therefore as toxic as Ag at the first time point in LB before toxicity patterns diverged. In AW, no toxicity was monitorable for ZnO NM-110, so no IC_{50} could be derived either. Consequently, toxic effects of ZnO NM-110 occurred exclusively and transiently in LB for the first hour of exposure along with cellular recovery over time as suggested by the relative luminescence reduction plots (Fig. 1, red curves) and supported by the derived IC_{50} values (Table 2). Comparatively, IC_{50} values for Zn ions (applied as zinc sulphate) evolved from 46.9 ± 6.6 mg L^{-1} to 73.3 ± 8.3 mg L^{-1} in LB during first hour of exposure and were not derived in AW as no toxicity was observed.

For TiO_2 NM-104, exposures at concentration up to 200 mg L^{-1} resulted in no detectable toxicity over time in either LB or AW (Fig. 1, green curves). Due to absence of detected toxicity, no IC_{50} could be derived.

3.2. Nanoparticle characterisation

Nanoparticle characterisation was carried out in both LB and AW by UV–vis (Fig. 2) and DLS (Fig. 3) to evaluate agglomeration status, as well as by AAS (Fig. 4) to quantify dissolution rates (*i.e.* the proportion of released ions from the nanoparticles).

As presented in Fig. 2A., Ag NM-300K showed characteristic and comparable UV–vis spectra with a unique and narrow peak in both matrices. Peak positions were observed at 413.6 ± 0.6 nm and 415.2 ± 0.3 nm with absorbance intensities of 1.06 ± 0.04 a.u. and 0.89 ± 0.02 a.u. in AW and LB, respectively. DLS data showed non-significantly different mean hydrodynamic sizes of 140 ± 7 nm in LB and 40 ± 1 nm in AW, in addition to the polydispersity of the material (PDI ~0.5) in both matrices (Fig. 3). AAS analyses indicated low and time independent dissolution rates of Ag NM-300K close to 4% in LB and to 2% in AW, which were not found significantly different either (Fig. 4A.). Consequently, Ag NM-300K showed comparable fates in LB and AW in terms of agglomeration and dissolution, which both appeared very low.

As shown in Fig. 2B., ZnO NM-110 exhibited characteristic (one peak close to 380 nm followed by a long tail) but non-comparable UV–vis spectra between matrices. Peak positions were observed at 374.8 ± 0.3 nm and 385.4 ± 4.5 nm with absorbance intensities of 2.0 ± 0.3 a.u. and 0.78 ± 0.8 a.u. in LB and AW, respectively. Significantly different mean hydrodynamic sizes of 177 ± 4 nm in LB and 1537 ± 265 nm in AW, in addition to the polydispersity of the material (PDI ~0.6) in both matrices (Fig. 3) were observed as well. AAS analyses indicated matrix dependent and time independent dissolution rates of ZnO NM-110 NPs close to 40% in LB and to 2.5% in AW (Fig. 4B.). Consequently, ZnO NM-110 exhibited non-comparable fates in LB and AW attesting overall to high aggregation and low dissociation phenomena in AW compared to LB.

As shown in Fig. 2C., TiO_2 NM-104 showed similar UV–vis spectra between matrices. Peak positions were observed at 325.1 ± 5.2 nm and 340.5 ± 6.8 nm with absorbance intensities of 0.38 ± 0.03 a.u. and 0.29 ± 0.02 a.u. in LB and AW, respectively. DLS data showed significantly different mean hydrodynamic sizes of 244 ± 8 nm in LB and 677 ± 11 nm in AW, in addition to the polydispersity of the material (PDI ~0.3) in both matrices (Fig. 3). No dissolution studies were carried out for TiO_2 NM-104 since it was not considered relevant (*i.e.* TiO_2 NM-104 is essentially non-soluble in aqueous media and did not exhibit detectable toxicity in our assays). Consequently, TiO_2 NM-104 showed non-comparable fates in LB and AW attesting to more aggregation in AW compared to LB.

4. Discussion

This study aimed to evaluate the suitability of the *Pseudomonas putida* BS566::luxCDABE bioreporter based approach for the screening of nanoparticle ecotoxicity in defined matrices (*i.e.* a nutrient rich undefined laboratory medium and an artificial wastewater) with three model inorganic nanoparticles (Ag NM-300K, ZnO NM-110 and TiO_2 NM-104), as a preliminary step before considering applications with more complex matrices such as real wastewaters. When applicable, ecotoxicity results were related to NP characterisation information, such as agglomeration status and dissolution rates assessed by DLS, UV–vis and AAS.

Overall, data presented here demonstrated higher toxicity of Ag NPs, followed by ZnO NPs and TiO_2 NPs with derived IC_{50} values at 1 h close to 4–5 mg L^{-1} in both matrices for Ag NPs, evolving from 60 mg L^{-1} to 100 mg L^{-1} in LB exclusively for ZnO NPs, and higher than 200 mg L^{-1} in both LB and AW for TiO_2 NPs. In addition, IC_{50} values of 0.3–0.4 mg L^{-1} for Ag ions in both matrices and between 50 and 70 mg L^{-1} for Zn ions in LB exclusively were also determined, attesting to the higher toxicity of ions compared to their NP counterparts. Toxicity of various inorganic NPs has been recently reviewed for different organisms. Regarding bacteria based information, Bondarenko et al. (2013) discussed median inhibitory concentrations of 7.1 mg L^{-1} for Ag NPs (over 46 studies), 3.3 mg L^{-1} for Ag ions (over 27 studies), 500 mg L^{-1} for ZnO NPs (over 15 studies) and 30 mg L^{-1} for ZnO ions (over 9 studies). Similarly, Chernousova and Epple (2013) reported the mode of Ag NP and ion toxicity values on prokaryotes in the range 1–10 mg L^{-1} (over 32 studies) and 0.1–1 mg L^{-1} (over 10 studies), respectively; whereas toxicity of TiO_2 NPs was generally reported above 200 mg L^{-1} when

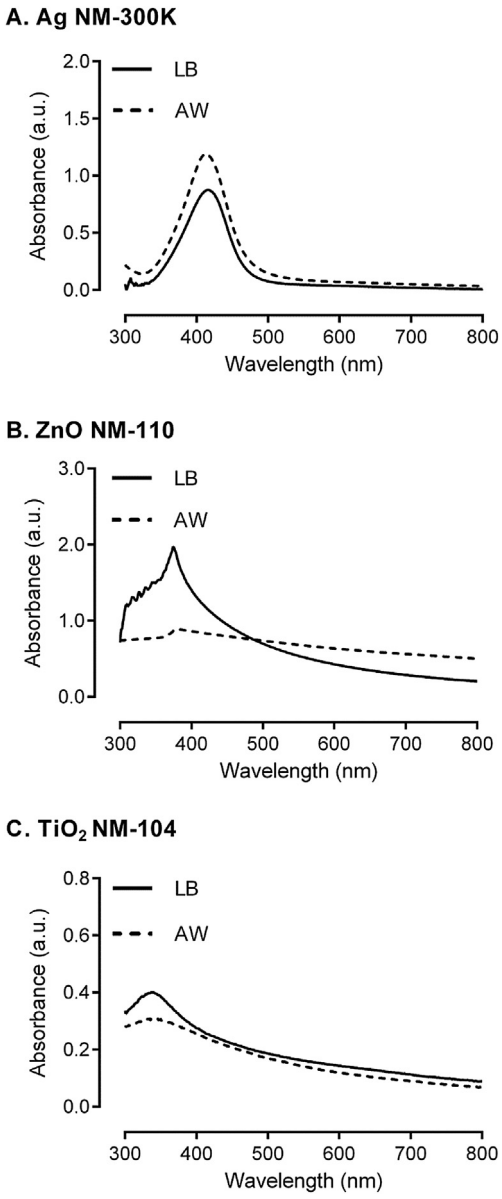

Fig. 2. Ag NM-300K, ZnO NM-110 and TiO_2 NM-104 characterisation by UV–visible in Luria Bertani (LB) medium and artificial wastewater (AW). Specific absorption spectra (from 300 nm to 800 nm) of 10 mg L^{-1} Ag (A.), 200 mg L^{-1} ZnO (B.) and 10 mg L^{-1} TiO_2 (C.) in both matrices (– LB and – AW, respectively). Spectra are typical examples of obtained results in each replicate.

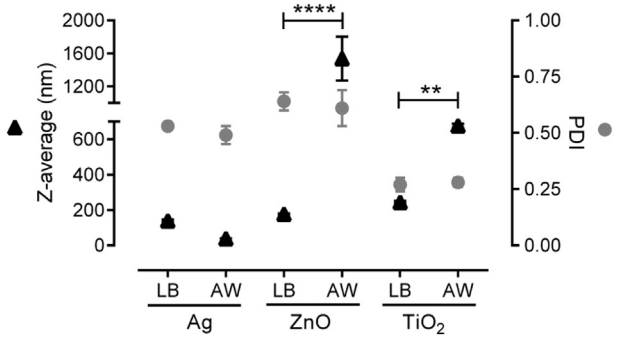

Fig. 3. Ag NM-300K, ZnO NM-110 and TiO_2 NM-104 characterisation by DLS in Luria Bertani (LB) medium and artificial wastewater (AW). Mean hydrodynamic size (z-average, Δ) and polydispersity index (PDI, ○) of 10 mg L^{-1} Ag, ZnO, and TiO_2 in both matrices (LB and AW). Data are mean ± standard error of the mean ($n = 3$). Significantly different at $^{**}p < 0.01$ and $^{****}p < 0.0001$.

observed (Suresh et al., 2013; von Moos and Slaveykova, 2014). Consequently, results presented here appear most of all directly in line with discussed nanoecotoxicological trends on various bacteria (despite differences in tested materials, used matrix of exposure or method of assessment amongst aforementioned information), attesting to the suitability of the used *P. putida* bioreporter.

Specifically regarding Ag NM-300K, results indicated comparable toxicity patterns in both LB and AW with main effects occurring during the very first stages of exposure. Although Ag NM-300K appeared toxic at slightly lower doses in AW (*i.e.* lower IC_{50} at 0 h, time point corresponding to the first measure registered in a 5 min time window after exposure of bacterial bioreporters to the nanoparticles) compared to LB, consistent IC_{50} values around 4–5 mg L^{-1} were derived over time in both matrices. Low dissolution rates were consistently observed over time and matrices and mean hydrodynamic sizes were not found significantly different either, as described elsewhere (Gaiser et al., 2013; Kermanizadeh et al., 2013). In addition, UV–vis spectra showing narrow and specific peaks very close to 413 nm would attest to the nanosize of Ag NM-300K preparations in both matrices (primary particle size <15 nm). Observed low agglomeration as well as consistent low dissolution and toxicity indicate that although ionic strength of AW was almost four times that of LB (~300 mM and ~80 mM, respectively, at pH 7), it was not instrumental in determining hazard over the full time period.

Dams et al. (2011) recently reported on *P. putida* BS566::luxCDABE bioreporter (in LB) higher toxicity of nano Ag compared to micro Ag as well as higher toxicity of nano Ag when dispersed, but they did not discuss the relative effect of released ions from particles. Obtained ionic silver (applied as silver nitrate) IC_{50} values ranged from 0.44 mg L^{-1} to 0.18 mg L^{-1} between 0.5 h and 1.5 h of exposure were however proposed. Considering in our case at 1 h a dissolution rate of ~4% and an IC_{50} of ~4 mg L^{-1} for Ag NM-300K in LB, we might estimate an ion based IC_{50} around 0.16 mg L^{-1}. Our own assays with Ag ions (applied as silver nitrate) led to a IC_{50} at 1 h between 0.3 and 0.4 mg L^{-1} in both matrices; results which are therefore directly comparable to previously published data (Dams et al., 2011). Consequently, Ag ions are at least one order of magnitude more toxic than the tested NP counterparts; observed Ag NM-300K toxicity is therefore likely to be driven by ion release, even at low dissolution rates, linked to the size of NPs as described elsewhere (Chernousova and Epple, 2013; Choi et al., 2008; Gaiser et al., 2013; Kermanizadeh et al., 2013; Sotiriou and Pratsinis, 2010), consistent for the different matrices. In addition, the toxicity of the same Ag NM-300K NPs and Ag ions was recently reported to be in the range 10–100 mg L^{-1} for a different bacterium, *Salmonella* spp. (Losasso et al., 2014). These authors concluded similarly, that dose-dependent effects occurred in the early stages of exposure for both NPs and ions with one order of magnitude of difference.

For ZnO NM-110, results indicated different toxicity patterns in both matrices. In LB ZnO NM-110 exhibited transient toxicity to *P. putida* BS566::luxCDABE, whereas, in AW no toxicity was observed. ZnO NPs are widely described to have high dissolution rates and to exhibit a toxicity mostly ion based (Kim and An, 2012; Li et al., 2011; Ma et al., 2013). Consequently, the detection of ZnO NM-110 toxicity in LB (*i.e.* IC_{50} between 60 and 100 mg L^{-1} during the first hour of exposure) might be at least partly associated to high dissolution rates (close to 40%) observed in this medium, whereas in contrast absence of toxicity in AW is likely to be linked to low dissolution rates (calculated as close to 2.5%). Dissolution of

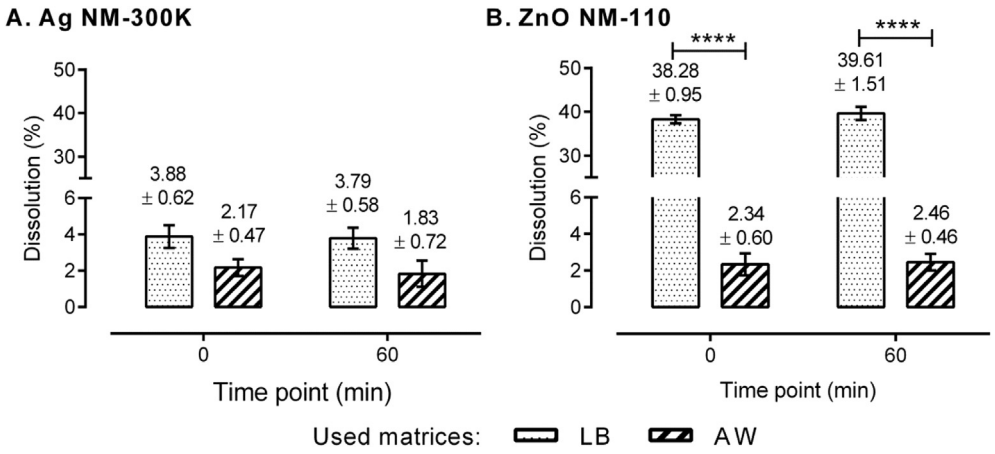

Fig. 4. Ag NM-300K and ZnO NM-110 characterisation by AAS in Luria Bertani (LB) medium and artificial wastewater (AW). Dissolution rates (%) of 50 mg L^{-1} of Ag (A.) and 200 mg L^{-1} of ZnO (B.) in LB and AW after 0 h or 1 h of incubation. Mean R^2 ± standard error obtained for AAS machine calibration between 0.156 mg L^{-1} and 5 mg L^{-1} were 0.9998 ± 0.0001 and 0.9880 ± 0.0010 for Ag and ZnO, respectively. Data are mean ± standard error of the mean with $n = 3$. Significantly different at ****$p < 0.0001$.

ZnO NPs is known as highly influenced by agglomeration, which tends to occur particularly in real waters and more generally under increasing ionic strength conditions (Keller et al., 2010; Li et al., 2011). DLS and UV–vis information confirmed occurring agglomeration in AW via higher z-average and non-comparable spectra between the two matrices. Consequently, final presence or absence of toxicity might likely be explained by the fate of ZnO NM-110 NPs leading, or not, to dissolution in each matrix governed mainly by ionic strength effects on the agglomeration status.

There is no comparable assessment of zinc oxide NPs or zinc ions on any similar *P. putida* bioreporters. However zinc ion toxicity on other bacteria species is reported to be in the range of 10–100 mg L^{-1} in laboratory media depending on NP type and size, matrix of exposure and method of assessment (Bondarenko et al., 2013; Suresh et al., 2013; Kim and An, 2012). Considering here a dissolution rate of 40% and IC_{50} values between 60 and 100 mg L^{-1} in LB, an ion based IC_{50} around 25–40 mg L^{-1} might be estimated. Our own assays with Zn ions (applied as zinc sulphate) led to transient toxicity (with IC_{50} evolving from about 50 to 70 mg L^{-1}) during the first hour of exposure in LB and to no toxicity in AW. Consequently, the observed ZnO NM-110 toxicity is likely to be driven by Zn ions and to be a transient phenomenon (in LB) as well as absence of toxicity (in AW) to be associated with readily occurring Zn ion complexation (with anions such as Cl^-, SO_4^{2-} and PO_4^{3-}) and/or precipitation in addition to Zn NP aggregation/precipitation between matrices, as reported in the literature (Kim and An, 2012; Li et al., 2011; Ma et al., 2013).

For TiO_2 NM-104, results indicated similar and non-detectable toxicity despite non-comparable NP fates in both matrices. TiO_2 NPs are however widely described to be toxic at high doses (up to the g L^{-1}) by the triggering of cellular oxidative stress pathways via their catalytic properties especially after photo-activation rather than by any ion based mechanisms (Bondarenko et al., 2013; Jiang et al., 2011; Keller et al., 2010; Kim and An, 2012; Shi et al., 2013; von Moos and Slaveykova, 2014). Non-detectable toxicity of TiO_2 NM-104 here might be therefore mainly explained by the concentrations used (up to 200 mg L^{-1}) and the absence of pre-photo-activation of materials. However, increasing concentrations or pre-activating materials, even if leading to monitorable toxicities, would not have been environmentally relevant thus was not explored. A TiO_2 dose-dependent increase in the output signal could be discussed, however as this occurs similarly from the first time point in both matrices this is likely to be associated with the intrinsic optical properties of TiO_2 (rutile form especially) to scatter and reflect light, as discussed elsewhere (Smijs and Pavel, 2011). Our own experiments using a luciferase based reaction with TiO_2 NM-104 (data not shown) support this. The following points should also be considered: 1) there is no comparable assessment of titanium dioxide NPs on similar *P. putida* bioreporters in the literature, and 2) not observing evident patterns via this *P. putida* bioreporter does not necessarily mean there was no stress based pathways triggered inside the cells. It does mean, however, this bioreporter (as all bioreporters) presented limitations when used on its own.

Modelled and measured environmental concentrations of Ag, ZnO and TiO_2 NPs ranging between 10^{-2}–10^{-3} μg L^{-1}, 10^{-2} μg L^{-1} and 10^{0}–10^{-1} μg L^{-1} in surface waters and 10^{-1}–10^{-2} μg L^{-1}, 10^{-2} μg $L^{-1}$and 10^{-1} μg L^{-1} in effluent wastewaters were recently reviewed and discussed by Gottschalk et al. (2013). Disregarding massive accidental or intentional discharges, there are still at least theoretically several orders of magnitude between expected or measured environmental concentrations of NPs and their threshold for toxicity (at least on bacteria). In addition, tested TiO_2 and ZnO NPs were not observed to be toxic in artificial wastewater following the experimental approach used in this study. Their environmental adverse effects might be therefore limited in real matrices as well. However, ZnO NPs were observed toxic in classical laboratory medium (*i.e.* LB), hence the importance to test in more realistic matrices and standardising suitable methods for this assessment, as stressed here. Ag NM-300K NPs showed consistent toxicity in both matrices, their adverse effect might be therefore more detrimental to the environment if released. It is likely that the tested Ag NPs were less subject to agglomeration and more protected from matrix effects due to being provided as suspension in a dispersant compared to the other NPs which were supplied as powders (Table 1). However, for industrial and commercial purposes, NPs are likely to be used (and ultimately released) in combination with dispersants or stabilisers in order to preserve or enhance their physico-chemical properties. Fate and toxicity of NPs following actual release from waste streams and industrial processes, etc. are likely to be different from their pristine counterparts especially when tested in laboratory media. Consequently, though located at the bottom of the aquatic food chain bacteria are unlikely to be the most dramatically affected at such modelled or measured concentrations. However, because of the advantages of using bacteria as bioreporters for environmental testing, they definitely offer relevant opportunities as high-throughput screening and patterning tools for standardised assessment of NPs in various matrices, including real and complex ones, as emphasised here.

5. Conclusions

Ecotoxicity of Ag NM-300K, ZnO NM-110 and TiO_2 NM-104 OECD model nanoparticles (as well as Ag and Zn ions) was assessed using a constitutively luminescent *P. putida* BS566::luxCDABE bioreporter based methodology in two defined matrices (LB and AW). Toxicity results were correlated with material type and matrix dependent nanoparticle and ion fate when applicable. Overall results showed:

- the reliability of the switch-off *P. putida* BS566::luxCDABE bioreporter based assay for nanoparticle ecotoxicity screening in both matrices such as LB and more environmentally relevant matrices such as AW;
- a global ecotoxicity ranking depending on the tested material type (*i.e.* with toxicity of Ag > ZnO > TiO_2 NPs) and form (*i.e.* with toxicity of ions > nanoparticles);
- the respectively consistent and inconsistent behaviour of tested Ag and ZnO NPs, closely associated with various underlying aggregation and dissolution phenomena as well as released ion fates between matrices;
- and the importance of matrix of exposure selection as results in more realistic matrices such as artificial or real wastewater matrices may vary from common microbiological ones.

This work therefore reports on the suitability of a *P. putida* luminescent bioreporter based approach for the screening of nanoparticle ecotoxicity in environmentally relevant matrices such as the artificial wastewater, combined with characterisation information, and leads toward assays in real and complex matrices such as wastewaters. Incorporated in battery test approach along with others bacterial bioreporters or integrated into field portable devices, such bacterial tools promise efficient assessment of potential risks and mechanisms associated with nanoparticle fate and toxicity.

Acknowledgements

We thank Heriot-Watt University (Edinburgh, UK) for providing FM with a James Watt scholarship, Prof Nick Christofi (Napier University, Edinburgh, UK) for donation of bacterial bioreporter *P. putida* BS566::luxCDABE, and Dr Birgit Gaiser (Heriot-Watt University, Edinburgh, UK) for reviewing the manuscript. The authors would like to acknowledge the European Union's Seventh Framework Programme [FP7 2007-2013] under EC-GA No. 263215 'MARINA', for the provision of the nanomaterials used in this study.

References

Aspray, T.J., Hansen, S.K., Burns, R.G., 2005. A soil-based microbial biofilm exposed to 2,4-D: bacterial community development and establishment of conjugative plasmid pJP4. FEMS Microbiol. Ecol. 54 (2), 317–327.
Bondarenko, O., Juganson, K., Ivask, A., Kasemets, K., Mortimer, M., Kahru, A., 2013. Toxicity of Ag, CuO and ZnO nanoparticles to selected environmentally relevant test organisms and mammalian cells in vitro: a critical review. Arch. Toxicol. 87 (7), 1181–1200.
Chernousova, S., Epple, M., 2013. Silver as antibacterial agent: ion, nanoparticle, and metal. Angew. Chem. Int. Ed. 52 (6), 1636–1653.
Choi, O., Deng, K.K., Kim, N.J., Ross, L., Surampalli, R.Y., Hu, Z.Q., 2008. The inhibitory effects of silver nanoparticles, silver ions, and silver chloride colloids on microbial growth. Water Res. 42 (12), 3066–3074.
Dams, R.I., Biswas, A., Olesiejuk, A., Fernandes, T., Christofi, N., 2011. Silver nanotoxicity using a light-emitting biosensor Pseudomonas putida isolated from a wastewater treatment plant. J. Hazard. Mater. 195, 68–72.
Deryabin, D.G., Aleshina, E.S., Efremova, L.V., 2012. Application of the inhibition of bacterial bioluminescence test for assessment of toxicity of carbon-based nanomaterials. Microbiology 81 (4), 492–497.
Di Paola, A., Garcia-Lopez, E., Marci, G., Palmisano, L., 2012. A survey of photocatalytic materials for environmental remediation. J. Hazard. Mater. 211, 3–29.
Eduok, S., Martin, B., Villa, R., Nocker, A., Jefferson, B., Coulon, F., 2013. Evaluation of engineered nanoparticle toxic effect on wastewater microorganisms: current status and challenges. Ecotoxicol. Environ. Saf. 95 (1), 1–9.
Gaiser, B.K., Hirn, S., Kermanizadeh, A., Kanase, N., Fytianos, K., Wenk, A., Haberl, N., Brunelli, A., Kreyling, W.G., Stone, V., 2013. Effects of silver nanoparticles on the liver and hepatocytes in vitro. Toxicol. Sci. 131 (2), 537–547.
Girotti, S., Ferri, E.N., Fumo, M.G., Maiolini, E., 2008. Monitoring of environmental pollutants by bioluminescent bacteria. Anal. Chim. Acta 608 (1), 2–29.
Gogoi, S.K., Gopinath, P., Paul, A., Ramesh, A., Ghosh, S.S., Chattopadhyay, A., 2006. Green fluorescent protein-expressing Escherichia coli as a model system for investigating the antimicrobial activities of silver nanoparticles. Langmuir 22 (22), 9322–9328.
Gottschalk, F., Sun, T.Y., Nowack, B., 2013. Environmental concentrations of engineered nanomaterials: review of modeling and analytical studies. Environ. Pollut. 181, 287–300.
Holden, P.A., Nisbet, R.M., Lenihan, H.S., Miller, R.J., Cherr, G.N., Schimel, J.P., Gardea-Torresdey, J.L., Univ, C., 2013. Ecological nanotoxicology: integrating nanomaterial hazard considerations across the subcellular, population, community, and ecosystems levels. Acc. Chem. Res. 46 (3), 813–822.
Hwang, E., Lee, J., Chae, Y., Kim, Y., Kim, B., Sang, B., Gu, M., 2008. Analysis of the toxic mode of action of silver nanoparticles using stress-specific bioluminescent bacteria. Small 4 (6), 746–750.
Jiang, G.X., Shen, Z.Y., Niu, J.F., Bao, Y.P., Chen, J., He, T.D., 2011. Toxicological assessment of TiO_2 nanoparticles by recombinant Escherichia coli bacteria. J. Environ. Monit. 13 (1), 42–48.
Ju-Nam, Y., Lead, J.R., 2008. Manufactured nanoparticles: an overview of their chemistry, interactions and potential environmental implications. Sci. Total Environ. 400 (1–3), 396–414.
Kahru, A., Ivask, A., 2013. Mapping the dawn of nanoecotoxicological research. Acc. Chem. Res. 46 (3), 823–833.
Keller, A.A., Wang, H.T., Zhou, D.X., Lenihan, H.S., Cherr, G., Cardinale, B.J., Miller, R., Ji, Z.X., 2010. Stability and aggregation of metal oxide nanoparticles in natural aqueous matrices. Environ. Sci. Technol. 44 (6), 1962–1967.
Kermanizadeh, A., Vranic, S., Boland, S., Moreau, K., Baeza-Squiban, A., Gaiser, B.K., Andrzejczuk, L.A., Stone, V., 2013. An in vitro assessment of panel of engineered nanomaterials using a human renal cell line: cytotoxicity, pro-inflammatory response, oxidative stress and genotoxicity. BMC Nephrol. 14, 12.
Kim, H.-A., Choi, Y.J., Kim, K.-W., Lee, B.-T., Ranville, J.F., 2012. Nanoparticles in the environment: stability and toxicity. Rev. Environ. Health 27, 175–179, 4, Sp. Iss. SI.
Kim, S.W., An, Y.J., 2012. Effect of ZnO and TiO_2 nanoparticles preilluminated with UVA and UVB light on Escherichia coli and Bacillus subtilis. Appl. Microbiol. Biotechnol. 95 (1), 243–253.
Klaine, S.J., Alvarez, P.J.J., Batley, G.E., Fernandes, T.F., Handy, R.D., Lyon, D.Y., Mahendra, S., McLaughlin, M.J., Lead, J.R., 2008. Nanomaterials in the environment: behavior, fate, bioavailability, and effects. Environ. Toxicol. Chem. 27 (9), 1825–1851.
Li, F.F., Lei, C.Y., Shen, Q.P., Li, L.J., Wang, M., Guo, M.L., Huang, Y., Nie, Z., Yao, S.Z., 2013. Analysis of copper nanoparticles toxicity based on a stress-responsive bacterial biosensor array. Nanoscale 5 (2), 653–662.
Li, M., Zhu, L.Z., Lin, D.H., 2011. Toxicity of ZnO nanoparticles to Escherichia coli: mechanism and the influence of medium components. Environ. Sci. Technol. 45 (5), 1977–1983.
Losasso, C., Belluco, S., Cibin, V., Zavagnin, P., Micetic, I., Gallocchio, F., Zanella, M., Bregoli, L., Biancotto, G., Ricci, A., 2014. Antibacterial activity of silver nanoparticles: sensitivity of different Salmonella serovars. Front. Microbiol. 26 (5), 227–245.
Ma, H.B., Williams, P.L., Diamond, S.A., 2013. Ecotoxicity of manufactured ZnO nanoparticles – a review. Environ. Pollut. 172, 76–85.
Marcoux, M.A., Matias, M., Olivier, F., Keck, G., 2013. Review and prospect of emerging contaminants in waste - key issues and challenges linked to their presence in waste treatment schemes: general aspects and focus on nanoparticles. Waste Manag. 33 (11), 2147–2156.
Martin, M.M.B., Perez, J.A.S., Fernandez, F.G.A., Sanchez, J.L.G., Lopez, J.L.C., Rodriguez, S.M., 2008. A kinetics study on the biodegradation of synthetic wastewater simulating effluent from an advanced oxidation process using Pseudomonas putida CECT 324. J. Hazard. Mater. 151 (2–3), 780–788.
Oomen, A.G., Bos, P.M.J., Fernandes, T.F., Hund-Rinke, K., Boraschi, D., Byrne, H.J., Aschberger, K., Gottardo, S., von der Kammer, F., Kuehnel, D., et al., 2014. Concern-driven integrated approaches to nanomaterial testing and assessment – report of the NanoSafety Cluster Working Group 10. Nanotoxicology 8 (3), 334–348.
Paterson, G., Macken, A., Thomas, K.V., 2011. The need for standardized methods and environmental monitoring programs for anthropogenic nanoparticles. Anal. Methods 3 (7), 1461–1467.
Peralta-Videa, J.R., Zhao, L.J., Lopez-Moreno, M.L., de la Rosa, G., Hong, J., Gardea-Torresdey, J.L., 2011. Nanomaterials and the environment: a review for the biennium 2008–2010. J. Hazard. Mater. 186 (1), 1–15.
Sadik, O.A., Zhou, A.L., Kikandi, S., Du, N., Wang, Q., Varner, K., 2009. Sensors as tools for quantitation, nanotoxicity and nanomonitoring assessment of engineered nanomaterials. J. Environ. Monit. 11 (10), 1782–1800.
Scown, T.M., van Aerle, R., Tyler, C.R., 2010. Review: do engineered nanoparticles pose a significant threat to the aquatic environment? Crit. Rev. Toxicol. 40 (7), 653–670.
Shi, H., Magaye, R., Castranova, V., Zhao, J., 2013. Titanium dioxide nanoparticles: a review of current toxicological data. Part. Fibre Toxicol. 10.

Shim, H., Hwang, B., Lee, S.S., Kong, S.H., 2005. Kinetics of BTEX biodegradation by a coculture of Pseudomonas putida and Pseudomonas fluorescens under hypoxic conditions. Biodegradation 16 (4), 319–327.
Smijs, T.G., Pavel, S., 2011. Titanium dioxide and zinc oxide nanoparticles in sunscreens: focus on their safety and effectiveness. J. Nanotechnol. Sci. Appl. 4, 95–112.
Sotiriou, G.A., Pratsinis, S.E., 2010. Antibacterial activity of nanosilver ions and particles. Environ. Sci. Technol. 44 (14), 5649–5654.
Suresh, A.K., Pelletier, D.A., Doktycz, M.J., 2013. Relating nanomaterial properties and microbial toxicity. Nanoscale 5 (2), 463–474.
van der Meer, J.R., Belkin, S., 2010. Where microbiology meets microengineering: design and applications of reporter bacteria. Nat. Rev. Microbiol. 8 (7), 511–522.
von Moos, N., Slaveykova, V.I., 2014. Oxidative stress induced by inorganic nanoparticles in bacteria and aquatic microalgae – state of the art and knowledge gaps. Nanotoxicology 8 (6), 605–630.
Wiles, S., Whiteley, A.S., Philp, J.C., Bailey, M.J., 2003. Development of bespoke bioluminescent reporters with the potential for in situ deployment within a phenolic-remediating wastewater treatment system. J. Microbiol. Methods 55 (3), 667–677.
Xu, T.T., Close, D.M., Sayler, G.S., Ripp, S., 2013. Genetically modified whole-cell bioreporters for environmental assessment. Ecol. Indic. 28, 125–141.
Zook, J.M., Long, S.E., Cleveland, D., Geronimo, C.L.A., MacCuspie, R.I., 2011. Measuring silver nanoparticle dissolution in complex biological and environmental matrices using UV-visible absorbance. Anal. Bioanal. Chem. 401 (6), 1993–2002.